INSTITUTE OF PHYSICS PUBLISHING JOURNAL OF PHYSICS G: NUCLEAR AND PARTICLE PHYSICS

J. Phys. G: Nucl. Part. Phys. **32** (2006) 609–628 doi:10.1088/0954-3899/32/5/002

The sensitivity of cosmic ray air shower experiments for excited lepton and leptoquark detection

M C Espírito Santo[1], A Onofre[1,2], M Paulos[1], M Pimenta[1,3], J C Romão[3] and B Tomé[1]

[1] LIP, Av. Elias Garcia, 14–1, 1000-149 Lisboa, Portugal
[2] Universidade Católica, Figueira da Foz, Portugal
[3] IST, Av. Rovisco Pais, 1049-001 Lisboa, Portugal

E-mail: pimenta@lip.pt

Received 18 October 2005
Published 31 March 2006
Online at stacks.iop.org/JPhysG/32/609

Abstract

In this paper, the sensitivity of present and planned very high energy cosmic ray experiments to the production of excited leptons and leptoquarks is estimated and discussed. These particles arise in composite models with substructure in the fermionic sector. Leptoquarks also arise naturally in models attempting the unification of the quark and lepton sectors of the standard model of particle physics. Such exotic particles could be produced in the interaction of high energy quasi-horizontal cosmic neutrinos with the atmosphere, originating extensive air showers observable in large cosmic ray experiments. Excited lepton production could occur via neutral and charged current processes, $\nu N \rightarrow \nu^* X$ and $\nu N \rightarrow \ell^* X$. The hadronic component X, and possibly part of the excited lepton decay products, would contribute to the detectable shower. A leptoquark could be produced via their direct coupling to a quark and a neutrino. The hadronic decay products of the leptoquark, and possibly its leptonic decay products, would be detectable.

1. Introduction

In this paper, the possibility of excited lepton and leptoquark searches in current (AGASA [1], Fly's Eye [2]) and future (Auger [3], EUSO [4], OWL [5]) very high energy cosmic ray experiments is discussed.

Compositeness is a never discarded hypothesis for explaining the complexity of the present fundamental particle picture. In models with substructure in the fermionic sector, excited fermion states [6] are expected, and leptoquarks [7], spin 0 or 1 particles providing a direct coupling between a quark and a lepton, may arise. In general, leptoquarks arise naturally in several models attempting the unification of the quark and lepton sectors of the standard model (SM) of particle physics.

 © 2006 IOP Publishing Ltd Printed in the UK

In the past few years many searches for these exotic particles were performed in the accelerators around the world [8, 9]. So far, no evidence for excited fermions or leptoquarks was found, and stringent limits were set at the electroweak scale. In fact, the couplings and masses of these particles are constrained indirectly by low energy experiment and by the precise measurement of the Z^0 width, and direct and indirect searches at accelerators have set constraints at higher energies. Whereas in ep collisions at HERA, leptoquarks could be s-channel produced, in all cases (ep, e^+e^- and hadron colliders) both excited leptons and leptoquarks could arise as t-channel mediators of SM-like processes. If light enough, they could be produced at accelerators as final state particles of specific processes. It should be noted that if t-channel processes are involved limits obtained at accelerators are valid for first family exotic particles only, as the initial beams involve first family charged leptons. Whenever this is not the case, it will be clearly stated in the discussion of the results.

The race for higher energies has new partners in present and future large cosmic rays experiments. These experiments, covering huge detection areas, are able to explore the high energy tail of the cosmic ray spectrum, reaching centre-of-mass energies orders of magnitude above those of man made accelerators. Although having poorer detection capabilities and large uncertainties on the beam composition and fluxes, cosmic ray experiments present a unique opportunity to look for new physics at scales far beyond the TeV.

Energetic cosmic particles interact with the atmosphere of earth originating extensive air showers (EAS) containing billions of particles. While cosmic particles with strong or electromagnetic charges are absorbed in the first layers of the atmosphere, neutrinos have a much lower interaction cross section and can easily travel large distances. Energetic cosmic neutrinos, although not yet observed and with very large uncertainties on the expected fluxes, are predicted on rather solid grounds [10]. Nearly horizontal neutrinos, seeing a large target volume and with negligible background from 'ordinary' cosmic rays, are thus an ideal beam to explore possible rare processes [11].

Excited leptons could be produced in the interaction of high energy quasi-horizontal cosmic neutrinos with the atmosphere via t-channel neutral and charged current processes, $\nu N \rightarrow \nu^* X$ and $\nu N \rightarrow \ell^* X$ (ν^* and ℓ^* representing neutral and charged excited leptons, respectively). The hadronic component X, and possibly part of the excited lepton decay products would originate an extensive air shower, observable by large cosmic ray experiments.

If the available energies are high enough, these cosmic neutrino interactions should also create the ideal conditions for the production of leptoquarks, with dominance of s-channel resonant production. The produced leptoquarks are expected to decay promptly into a quark and a charged or neutral lepton. The branching ratio into the charged and neutral decay mode depends on the leptoquark type.

As the initial beam must contain all three neutrino flavours, one expects the production of excited leptons and leptoquarks of the first, second and third family. In the specific case of the third family excited leptons or leptoquarks decaying into τX, the subsequent decay of the tau lepton may originate a second visible air shower within the acceptance of the experiment and thus giving rise to a double bang event topology [12–14].

This paper is organized as follows. In section 2, the effective models used to describe excited leptons and leptoquarks are introduced. The production cross sections are obtained and the decay branching ratios at the relevant energies and masses are discussed. In section 3 the expected sensitivity to these exotic events of the largest available and planned cosmic ray experiments is estimated and discussed. Some conclusions are finally drawn.

2. Exotic particle production and decay

2.1. Excited leptons

The $SU(2)\times U(1)$ gauge invariant effective Lagrangian describing the magnetic transition between excited leptons and the standard model (SM) leptons has the form [6]

$$\mathrm{L}_{ll^*} = \frac{1}{2\Lambda}\overline{L^*}\sigma^{\mu\nu}\left[gf\frac{\boldsymbol{\tau}}{2}\mathbf{W}_{\mu\nu} + g'f'\frac{Y}{2}B_{\mu\nu}\right]L_L + \mathrm{h.c.} \tag{1}$$

where $L^* = L_L^* + L_R^*$, with

$$L_L^* = \begin{bmatrix}\nu^*\\ \ell^*\end{bmatrix}_L, \qquad L_R^* = \begin{bmatrix}\nu^*\\ \ell^*\end{bmatrix}_R$$

and L_L is the weak isodoublet with the left-handed components of the SM leptons. Above, $\sigma^{\mu\nu}$ is the covariant bilinear tensor, $\boldsymbol{\tau}$ are the Pauli matrices, Y is the weak hypercharge, $\mathbf{W}_{\mu\nu}$ and $B_{\mu\nu}$ represent the gauge field tensors of $SU(2)$ and $U(1)$, respectively, and g and g' are the corresponding SM coupling constants. The parameter Λ sets the compositeness scale and f, f' are weight factors associated with the two gauge groups.

This Lagrangian describes the ll^*V vertex, with $V = \gamma, \mathrm{Z}^0, \mathrm{W}^\pm$, and thus the single production of excited leptons and their decays. The strength of the ll^*V coupling is parameterized through f and f'. Form factors and anomalous magnetic moments of the excited leptons were not considered. From this Lagrangian we can derive the vertex

$$\Gamma_\mu^{Vl^*l} = \frac{e}{2\Lambda}q^\nu\sigma_{\mu\nu}(1-\gamma_5)f_V$$

where the couplings to the physical gauge bosons are

$$f_\gamma = e_l f' + I_{3L}(f - f'), \qquad f_W = \frac{1}{\sqrt{2}s_W}f, \qquad f_Z = \frac{I_{3L}\left(c_W^2 f + s_W^2 f'\right) - e_l s_W^2 f'}{s_W c_W},$$

I_{3L} being the fermion weak isospin and $s_W = \sin\theta_W$, $c_W = \cos\theta_W$, with θ_W the SM weak mixing angle. To reduce the number of free parameters, it is customary to assume a relation between f and f'. In this paper, the scenarios $f = f'$ and $f = -f'$ will be considered. In these cases, the single excited lepton production cross section depends only on the ratio $|f|/\Lambda$ and on the excited lepton mass. It is worth noting that, for $f = f'$, the coupling of the excited neutrinos to the photon vanishes. The same is true for excited charged leptons if $f = -f'$.

2.1.1. Production. The production of excited leptons in neutrino–parton collisions is described at the lowest order by the t-channel exchange of a $\mathrm{W}^\pm$ boson, in the case of excited charged lepton production (charged current, CC), or of a Z^0 boson, for excited neutrino production (neutral current, NC). In the case of the neutral currents, an additional contribution from t-channel γ exchange arises in scenarios with $f \neq f'$, due to the non-vanishing coupling to the photon. The tree level diagrams are shown in figure 1.

From the above Lagrangian, the differential cross section for neutrino–parton interactions can be written as

$$\frac{\mathrm{d}\sigma_{\nu q}}{\mathrm{d}Q^2}(\hat{s}, Q^2) = 2\pi\alpha^2\left(\frac{f}{\Lambda}\right)^2 Q^2[D_l(Q^2)S(\hat{s}, Q^2) \pm \bar{D}_l(Q^2)A(\hat{s}, Q^2)], \tag{2}$$

where the plus and minus signs apply to partons and antipartons, respectively, $-Q^2$ is the momentum transfer, $\hat{s}$ is the parton level centre-of-mass energy and

$$S(\hat{s}, Q^2) = 2 - (2-r)\left(\frac{Q^2}{\hat{s}} + r\right), \qquad A(\hat{s}, Q^2) = r\left(2 - \frac{Q^2}{\hat{s}} - r\right),$$

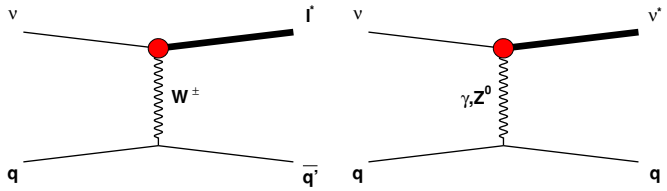

Figure 1. Lowest order Feynman diagrams for the single production of excited leptons in neutrino–quark collisions via charged current (left) and neutral current (right) interactions. The vertex shown as a closed circle represents a ll^*V coupling ($V \equiv \gamma, \mathrm{W}^{\pm}, \mathrm{Z}^0$) proportional to $1/\Lambda$. The t-channel photon exchange can only occur in scenarios with $f \neq f'$.

where $r \equiv m_*^2/\hat{s}$ and m_*^2 is the excited lepton mass. In the case of charged excited lepton production via CC, the D_l, $\bar{D}_l$ functions can be written as

$$D_e = \bar{D}_e = \left(\frac{f_W}{f}\right)^2 \frac{a_W^2 + v_W^2}{\left(Q^2 + M_W^2\right)^2}.$$

For excited neutrino production via NC, both the Z^0 and the γ contribution have to be taken into account and the D_l, $\bar{D}_l$ can be written as follows:

$$D_\nu = \frac{e_q^2}{(Q^2)^2}\left(\frac{f_\gamma}{f}\right)^2 + \frac{2e_q v_q^Z}{Q^2\left(Q^2 + M_Z^2\right)}\left(\frac{f_\gamma f_Z}{f}\right)^2 + \frac{\left[\left(v_q^Z\right)^2 + \left(a_q^Z\right)^2\right]}{\left(Q^2 + M_Z^2\right)^2}\left(\frac{f_Z}{f}\right)^2$$

$$\bar{D}_\nu = \frac{2e_q a_q^Z}{Q^2\left(Q^2 + M_Z^2\right)}\left(\frac{f_\gamma f_Z}{f}\right)^2 + \frac{2v_q^Z a_q^Z}{\left(Q^2 + M_Z^2\right)^2}\left(\frac{f_Z}{f}\right)^2.$$

In the expressions above, the SM couplings are

$$a_W = v_W = \frac{1}{2\sqrt{2}s_W}, \qquad v_q^Z = \frac{2I_{3L}^q - 4e_q s_W^2}{4c_W s_W}, \qquad a_q^Z = \frac{2I_{3L}^q}{4c_W s_W},$$

where I_{3L}^q is the quark weak isospin.

The double differential deep inelastic scattering (DIS) neutrino–nucleon cross sections can be written as

$$\frac{\mathrm{d}^2\sigma_{\nu N}}{\mathrm{d}x\,\mathrm{d}y} = \sum_q q(x, Q^2)\frac{\mathrm{d}\sigma_{\nu q}}{\mathrm{d}y}\bigg|_{\hat{s}=xs} = \sum_q q(x, Q^2)xs\frac{\mathrm{d}\sigma_{\nu q}}{\mathrm{d}Q^2}\bigg|_{\hat{s}=xs}$$

$$= 2\pi\alpha^2\left(\frac{f}{\Lambda}\right)^2 (xs)^2 y\sum_q [D_l(Q^2)S(x, y) \pm \bar{D}_l(Q^2)A(x, y)]q(x, Q^2), \tag{3}$$

where $y = (E_\nu - E^*)/E_\nu$ is the inelasticity parameter (E_ν is the incident neutrino energy and E^* is the excited lepton energy), $x = Q^2/sy$ is the Bjorken variable, $q(x, Q^2)$ are the quark distribution functions and the sum runs over the quark types. We neglect the top distribution function, but we take into account the threshold suppression of the $b \to t$ transition, using the standard 'slow-rescaling' prescription [15]. In this work, the CTEQ6-DIS parton distribution functions [16] were used.

The total CC or NC production cross sections will thus be given by

$$\sigma_{\nu N}(eN \to l^* X) = \int_{(m_*^2+Q_0^2)/s}^1 \mathrm{d}x \int_{Q_0^2/xs}^{1-r} \mathrm{d}y \frac{\mathrm{d}^2\sigma_{\nu N}}{\mathrm{d}x\,\mathrm{d}y} + \sigma_{\mathrm{el}} + \sigma_{\mathrm{low}}, \tag{4}$$

where the first term is the deep inelastic scattering (DIS) contribution, and $\sigma_{\rm el}$ and $\sigma_{\rm low}$ are the elastic and low inelastic contributions, respectively. These last two terms will only be important in the case $f = -f'$, which will be discussed below. The integration limits arise from kinematic considerations and from taking the parton model as valid for $Q^2 > Q_0^2 \simeq 5\ \mathrm{GeV}^2$.

At the energies of interest, the propagator damps the cross section for high enough x, effectively limiting its value to $x \leqslant M_W^2/s \simeq 10^3\ \mathrm{GeV}/E(\mathrm{GeV})$. For energies above 10^9 GeV, we are probing values of x well below the available data. There are several approaches for extrapolating the parton distribution functions, recently reviewed in [17]. This leads to an uncertainty in the SM neutrino cross section predictions of about a factor 2 for the highest energies. In this paper we extrapolate below $x = 10^{-6}$ as described in [17], that is, by matching

$$x\bar{q}(x, Q) = \left(\frac{x_{\rm min}}{x}\right)^{\lambda} x\bar{q}(x_{\rm min}, Q).$$

With this method we reproduce the results for the SM neutrino–nucleon cross section as obtained in [18] within 10%. It should be noted, however, that the uncertainty in the extrapolations is much lower in the present case than in the SM, in the light of two reasons. One is the kinematic constraint $x > m_*^2/s$, which, for example, at $m_* = 1\ \mathrm{TeV}/c^2$ and $E = 10^{12}$ GeV leads to x well within the available region in CTEQ6. The other is the x^2 dependence of the cross section, as opposed to the SM linear dependence, damping the low x contributions.

In the scenario $f = -f'$, the NC photon exchange diagram is also present, and the low Q^2 nucleon–parton interactions have to be taken into account. The differential cross section can be written in terms of the proton structure functions F_1 and F_2, and both the elastic and inelastic contributions were taken into account. In the elastic case, standard proton structure functions as described, for example, in [6] were used. In the inelastic case, the parameterization of the structure functions described in [19] was taken.

It should however be noted that the low Q^2 region is in the present case not as relevant as in [6]. In fact, provided we are well above the kinematic limit for excited lepton production, the DIS contribution to the cross section is largely dominant. However, these effects become relevant near the threshold and have to be taken into account. With the cross-section changes corresponding to the $ep \to l^*X$ case, we were able to reproduce the results in [6].

The total production cross section as a function of the incident neutrino energy is shown in figure 2(a), for both the charged and neutral current processes, with $f/\Lambda = 15\ \mathrm{TeV}^{-1}$ and a chosen value of the excited lepton mass. The total SM νN cross section is also shown for comparison. In figure 2(b), the total cross section is shown as a function of the excited lepton mass, for $f/\Lambda = 15\ \mathrm{TeV}^{-1}$ and a chosen value of the neutrino energy. In both figures, the elastic and low Q^2 inelastic contributions to the NC, $f = -f'$ cross section are shown separately.

In figure 3, the differential cross sections

$$\frac{\mathrm{d}\sigma_{\nu N}}{\mathrm{d}y} = \int \mathrm{d}x \frac{\mathrm{d}^2\sigma_{\nu N}}{\mathrm{d}x\,\mathrm{d}y} \tag{5}$$

are shown as an example for fixed values of the incident neutrino energy and of the excited lepton mass and coupling parameters. The charged current cross section is shown, together with the neutral current cross sections for $f = f'$ and $f = -f'$. In the latter, the elastic and low Q^2 inelastic contributions are visible, in the lowest and intermediate range of $\log_{10}(y)$, respectively.

These distributions determine the fraction of the incident neutrino energy carried away by the hadronic component X and thus, to some extent, the energy of the observable extensive

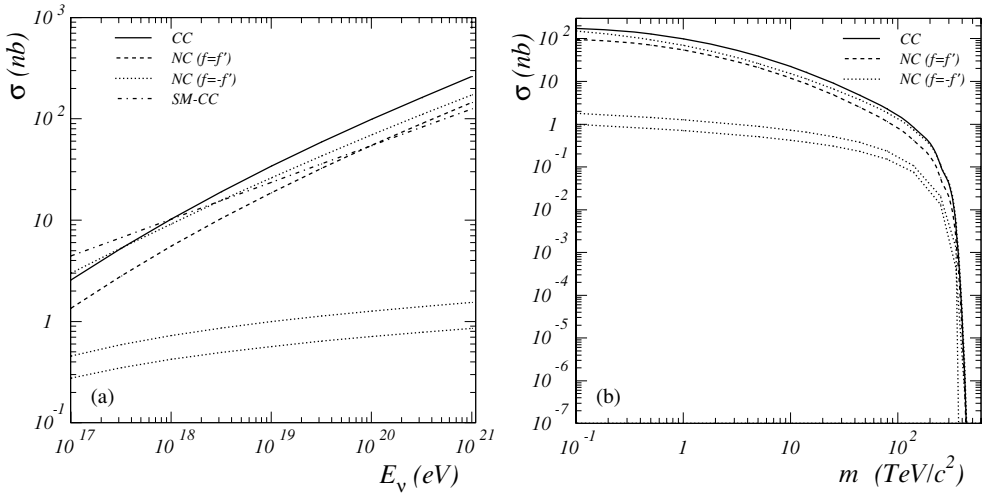

Figure 2. Excited lepton production cross section in νN collisions, via charged and neutral current interactions, with $f/\Lambda = 15$ TeV^{-1} (a) as a function of the incident neutrino energy for $m_* = 1$ TeV$/c^2$ and (b) as a function of the excited lepton mass for $E_\nu = 10^{20}$ eV. The lower dotted curves show separately the elastic (upper) and inelastic low Q^2 (lower) contributions to the NC $f = -f'$ cross section. In (a) the SM neutrino–nucleon CC cross section is also shown for comparison.

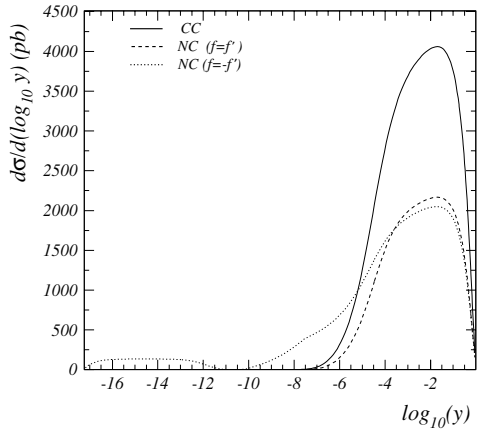

Figure 3. Differential excited lepton production cross section in charged and neutral current νN interactions with $f/\Lambda = 15$ TeV^{-1}, $E_\nu = 10^{20}$ eV and $m_* = 14$ TeV$/c^2$. For NC and $f = -f'$, the elastic and low Q^2 inelastic contributions are visible in the lowest and intermediate range of $\log_{10}(y)$, respectively.

air shower. The observability of the excited lepton decay products will depend on the decay mode, as discussed in detail in section 3.

2.1.2. Decay. Excited leptons are assumed to decay promptly by radiating a γ, $W^{\pm}$ or Z^0 boson. For $\Lambda = 1$ TeV and $E < 10^{21}$ eV, their decay length is predicted to be less than 10^{-4} m and, in all the studied scenarios, they decay essentially at the production point. The decay

branching ratios are also functions of the f and f' parameters. While at lower masses the branching ratios show an important dependence on the excited lepton mass, they are practically constant in the interesting mass range ($m_* > 200\ \mathrm{GeV}/c^2$). For charged excited leptons, the electromagnetic radiative decay is forbidden if $f = -f'$ and the decays proceed exclusively through Z^0 and $\mathrm{W}^\pm$ bosons, with branching fractions of about 40% and 60%, respectively. However, as long as $f \neq -f'$, there is a significant contribution to the total decay width from the electromagnetic radiative decay, even if the difference $|f| - |f'|$ is much smaller than $|f|$. In the $f = f'$ case, the electromagnetic radiative decay is largely dominant at masses below the $\mathrm{W}^\pm$, Z^0 gauge boson masses. In the presently interesting mass range, the decay into the $\mathrm{W}^\pm$ is again about 60%, while the branching ratios of the decays through a photon or a Z^0 are of the order of 30% and 10%, respectively. Conversely, for neutral excited leptons the electromagnetic radiative decay is forbidden if $f = f'$.

2.2. Leptoquarks

Leptoquarks are coloured spin 0 or spin 1 particles with non-zero baryon and lepton quantum numbers. They are predicted by different extensions of the SM. In this paper, we follow the conventions and theoretical framework formulated in [7], where the most general $SU(3) \times SU(2) \times U(1)$ invariant Lagrangian is given for each family as

$$\begin{aligned}\mathcal{L} = {} & \left(g_{1L}\bar{q}_L^c \mathrm{i}\tau_2 \ell_L + g_{1R}\bar{u}_R^c e_R\right) S_1 + \tilde{g}_{1R}\bar{q}_R^c e_E \tilde{S}_1 + g_{3L}\bar{q}_L^c \mathrm{i}\tau_2 \boldsymbol{\tau} \ell_L S_3 \\ & + \left(g_{2L}\bar{d}_R^c \gamma^\mu \ell_L + g_{2R}\bar{q}_L^c \gamma^\mu e_R\right) V_{2\mu} + \tilde{g}_{2L}\bar{u}_R^c \gamma^\mu \ell_L \tilde{V}_{2\mu} + \tilde{h}_{2L}\bar{d}_R \ell_L \tilde{R}_2 \\ & + (h_{2L}\bar{u}_R \ell_L + h_{2R}\bar{q}_L \mathrm{i}\tau_2 e_R) R_2 + (h_{1L}\bar{q}_L \gamma^\mu \ell_L + h_{1R}\bar{d}_R \gamma^\mu e_R) U_{1\mu} \\ & + \tilde{h}_{1R}\bar{u}_R \gamma^\mu e_R \tilde{U}_{1\mu} + h_{3L}\bar{q}_L \boldsymbol{\tau} \gamma^\mu \ell_L U_{3\mu} + \mathrm{h.c.} \end{aligned} \tag{6}$$

We can see that there are 18 leptoquarks per family: nine scalars and nine vectors. We also note that some of these are grouped into weak isospin doublets or triplets, which are referred to by their indices (1 for scalar, 2 for doublet, 3 for triplet). As in [7], we assume that the couplings are diagonal in generation space.

It is assumed that only one of the chiral coupling constants is non-zero. In the case of ep collisions, it was shown [7] that qualitatively similar results could be obtained either by taking $\lambda_R = 0$ or $\lambda_L = 0$, where λ represents the coupling relevant to the leptoquark in question ($g_i, \tilde{g}_i, h_i, \tilde{h}_i$) as defined in equation (6). However, for νp collisions, only the case $\lambda_L \neq 0$ is of interest, otherwise the neutrino will not couple to the leptoquarks. So in the following we consider $\lambda_R = 0$. From the above Lagrangian we can easily derive the decay modes and coupling constants for neutrino induced leptoquark production. This is shown in table 1, where the listed leptoquarks can be of the first, second or third family (family indices are omitted) and $D = d, s, b$ and $U = u, c$, as we neglect the top parton distribution function (PDF). Unless explicitly stated, in all our results we consider the leptoquarks for which the factor $\sqrt{2}$ in the couplings is not present. For the other leptoquarks the results can be obtained by a simple rescaling. In the table, the possible decay modes (charged and neutral or neutral only) of each leptoquak type are also indicated.

The processes shown in table 1 can thus occur for leptoquarks of the first, second or third family. For our range of energies we are probing very small values of x and the cross sections are comparable for the three families. In the following, first family leptoquarks will sometimes be taken as a case study, but all families will be considered in the result derivation.

All the processes in table 1 occur by the s-channel. However, flipping the quark to antiquark in each case leads to an alternative reaction, this time mediated by a u-channel

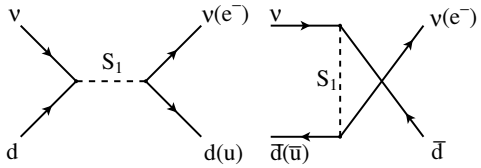

Figure 4. Lowest order Feynman diagrams for leptoquark production in neutrino–quark collisions via s-channel (left) and u-channel (right) interactions (the specific case of S_1 leptoquarks is shown).

Table 1. Relevant processes for neutrino induced leptoquark production, assuming $\lambda_R = 0$. Here $D = d, s, b$, $U = u, c$, $\ell = e, \mu, \tau$ and $\nu = \nu_e, \nu_\mu, \nu_\tau$.

Leptoquark	Interaction	Decay	Coupling
		Scalars	
S_1	νD	$\nu D, \ell^- U$	$-g_{1L}, g_{1L}$
S_3^3	νD	$\nu D, \ell^- U$	$-g_{3L}, -g_{3L}$
S_3^-	νU	νU	$\sqrt{2}g_{3L}$
R_2^U	$\nu \bar{U}$	$\nu \bar{U}$	h_{2L}
$\tilde{R}_2^U$	$\nu \bar{D}$	$\nu \bar{D}$	$\tilde{h}_{2L}$
		Vectors	
$V_{2\mu}^U$	νD	νD	g_{2L}
$\tilde{V}_{2\mu}^U$	νU	νU	$\tilde{g}_{2L}$
$U_{1\mu}$	$\nu \bar{U}$	$\nu \bar{U}, \ell^- D$	h_{1L}, h_{1L}
$U_{3\mu}^3$	$\nu \bar{U}$	$\nu \bar{U}, \ell^- \bar{D}$	$h_{3L}, -h_{3L}$
$U_{3\mu}^-$	$\nu \bar{D}$	$\nu \bar{D}$	$\sqrt{2}h_{3L}$

leptoquark exchange, as is shown in figure 4. All the relevant amplitudes are given explicitly in [7] for eq interactions and can easily be adapted to our νq case, so we will not repeat them here. The contribution from s-channel resonant production is largely dominant up to moderate values of λ. In fact, for values $\lambda \leqslant 5$, the width is small compared with the leptoquark mass and the differential cross section is strongly peaked on the x value corresponding to the resonance pole, $x = m_{LQ}^2/s$, which gives the main contribution to the total cross section. For this range of λ, the narrow width approximation [7]

$$\sigma(\nu p \to LQ) = \frac{\pi}{4s}\lambda^2 q\left(\frac{m_{LQ}^2}{s}\right) \times C_J \qquad C_J = 1, 2 \qquad \text{for} \quad J = 0, 1 \tag{7}$$

explains why the cross section rises like λ^2, as is shown in figure 5. However, for larger values of λ, the narrow width approximation can no longer be used and the dependence of the cross section with λ begins to flatten out, depending on the energy of the incident neutrino. For these larger values of λ, the u-channel is no longer negligible and has to be taken in account. Also, the leptoquarks with one or two decay modes, indistinguishable in the narrow width approximation, start to separate for larger values of λ. In figure 6 we plot the total cross section as a function of the energy for different values of λ. As we intend to obtain sensitivities for values of λ that can be above the conditions of applicability of the narrow

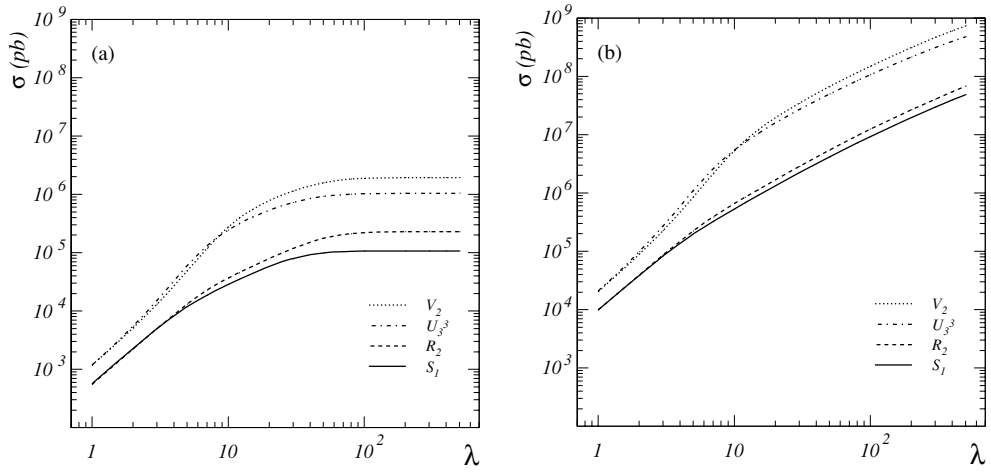

Figure 5. Total cross sections for scalar and vector leptoquarks as a function of the coupling λ for $M_{LQ} = 1$ TeV and two different neutrino energies: (a) $E_\nu = 10^{17}$ eV, (b) $E_\nu = 10^{20}$ eV. The upper (lower) lines correspond to vector (scalar) leptoquarks.

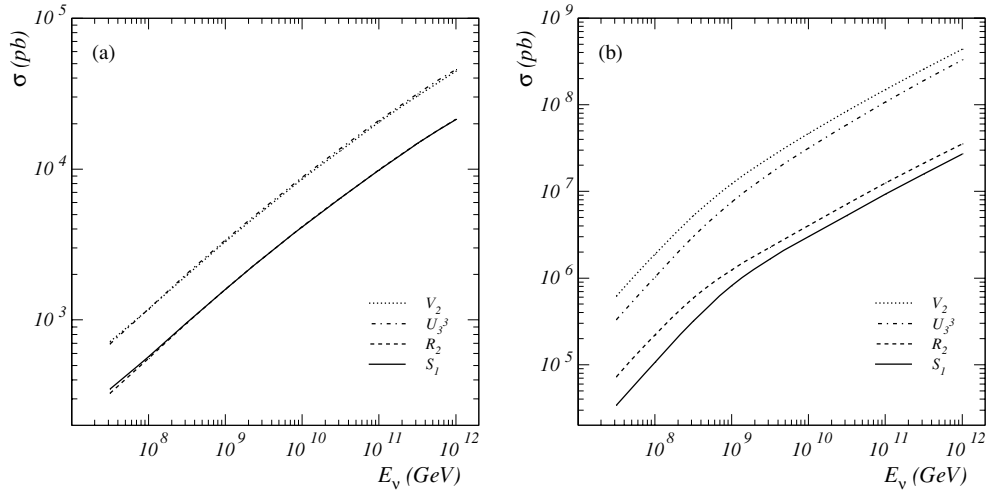

Figure 6. Total cross sections for scalar and vector first family leptoquarks as a function of energy for $M_{LQ} = 1$ TeV and two different values of λ: (a) λ = 1 and (b) λ = 100.

width approximation, in this work we always performed the complete calculations, without any approximation.

The dependence of the total cross section on the leptoquark mass is shown in figure 7 for a scalar and a vector leptoquark. The curves corresponding to other scalars (or vectors) of the same family are identical to these two.

All the figures above correspond to first family leptoquarks. In figure 8 a comparison of the total cross section for the leptoquark S_1 of different families is shown as a function of incident neutrino energy. As expected, the observed differences are attenuated when the energy increases, as mass effects become less relevant.

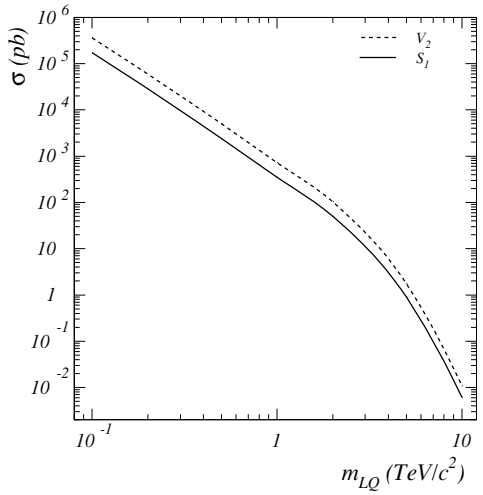

Figure 7. Total cross sections for scalar and vector first family leptoquarks as a function of the leptoquark mass for $E = 10^{20}$ eV and $\lambda = 1$.

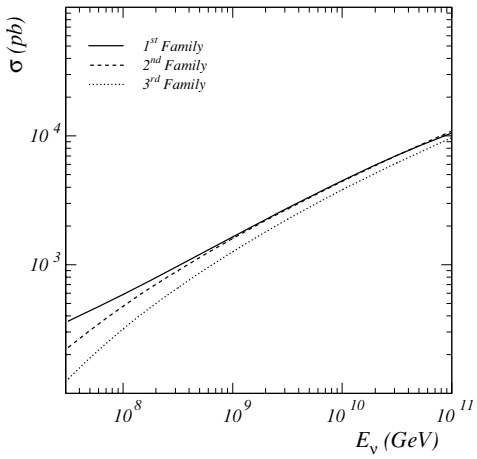

Figure 8. Total cross sections for S_1 leptoquarks of different families as a function of the incident neutrino energy for $M_{LQ} = 1$ TeV and $\lambda = 1$.

3. Limits and sensitivities

The expected number of observed exotic events is given by

$$\mathtt{N} = N_A \int \frac{\mathrm{d}\phi_\nu}{\mathrm{d}E_\nu} \sigma_{\nu N} \mathtt{A} \Delta T \, \mathrm{d}E_\nu, \tag{8}$$

where $\mathrm{d}\phi_\nu/\mathrm{d}E_\nu$ is the incident neutrino flux, $\sigma_{\nu N}$ is the production cross section for the considered exotic channel (depending on the leptoquark type, or on whether neutral or charged excited lepton production is considered), $\mathtt{A}$ is the acceptance of the experiment for the extensive air showers produced by these final states, ΔT is the observation time interval and N_A is Avogrado's number. For simplicity, it is assumed that the attenuation of neutrinos in the atmosphere can be neglected. This is a reasonable assumption in most of the cross-section ranges relevant for the present study. In fact, following the treatment in [20], negligible attenuation factors are expected for cross sections up to 1 μbarn. In the case of leptoquarks (see section 2.2) larger cross sections may arise for large primary energies ($E \sim 10^{20}$ eV) and very large couplings ($\lambda \sim 100$). For primary neutrinos up to about 85° incidence in polar angle, the attenuation factors are still below 30%. Beyond, the treatment discussed in [20] should be applied.

The estimation of the different factors in the expression is discussed below.

In this work the Waxman–Bahcall (WB) [21, 22] bound with no z evolution, $E_\nu^2 \frac{\mathrm{d}\phi}{\mathrm{d}E_\nu} = 10^{-8}$ (GeV cm^{-2} s^{-1} sr^{-1}) is assumed. This flux is much lower than the cascade [23] or the Mannheim–Protheroe–Rachen upper bounds [22] and is, in the relevant neutrino energy range, higher but of the same order of magnitude of the 'best prediction' computation for cosmogenic neutrinos presented in [20]. Taking into account the existence of neutrino oscillations over cosmological distances, equal flux (one third of the WB flux) for each neutrino flavour was considered.

The neutral and charged current excited lepton production cross sections in neutrino–nucleon collisions are the ones computed in section 2.1.1. Similarly, the production cross sections for leptoquarks of different types are the ones obtained in section 2.2.

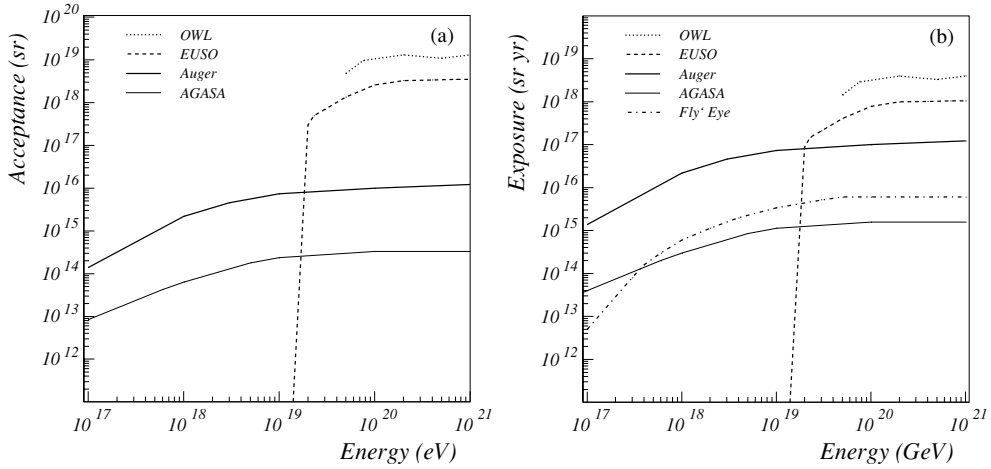

Figure 9. (a) Acceptances and (b) exposures of air shower cosmic ray experiments as a function of the final state extensive air shower energy. The information in [24–27] was used. The observation times were taken as 10 years for Auger, 3 years and 10% duty cycle for both EUSO and OWL. It should be noted that the relation between the shower energy and the incident neutrino energy is process dependent.

The observation times were assumed to be 10 years for Auger, 3 years and 10% duty cycle for both EUSO and OWL. For Agasa and Fly's Eye, the exposure was taken from [24].

3.1. Acceptance

The acceptance A(E) in equation (8) includes both the geometrical aperture, the target density and the detection efficiency factors:

$$\mathtt{A(E)} = \int \rho(\ell) A(E) \cos\theta \epsilon(E) \Delta\Omega \, \mathrm{d}\ell,$$

where $A(E)\cos\theta$ is the effective area, $\rho(\ell)$ the atmospheric density profile, $\epsilon(E)$ a global detection efficiency factor and $\Delta\Omega$ the observation solid angle. Under similar assumptions, acceptances have been computed for different experiments in the context of the estimation of the sensitivity for cosmic neutrinos [24–27]. It should be noted that, whereas these acceptances are valid for any νN interaction process, the relation between the shower energy and the primary neutrino energy is process dependent. Taking the SM as an example, whereas in the charged current process $\nu_e N \to eN$ the energy of the observed extensive air shower corresponds to the energy of the incident neutrino, this is not the case for the remaining neutrino families and for the neutral current case, $\nu N \to \nu N$, in which the final state neutrino goes undetected. The fraction of the primary energy that goes into EAS energy in the SM NC process is of the order of 20% for energies around 10^{19} eV, and decreases slowly with energy. It is thus convenient for the present purposes to plot the neutrino acceptances of the different experiments as a function of the shower energy. These acceptances are compiled in figure 9(a). For Auger, the most conservative estimate of the acceptance for quasi-horizontal showers as determined by Monte Carlo simulations [25] was considered. The acceptance of AGASA was conservatively taken as the acceptance for electromagnetic showers given in [24]. A discussion of the acceptance of AGASA for hadronic and electromagnetic showers can be found in [20]. The acceptance of EUSO was taken from the estimation in [26], including the trigger and visibility of the shower maximum conditions but no cloud effect (which was included as a reduction of the duty

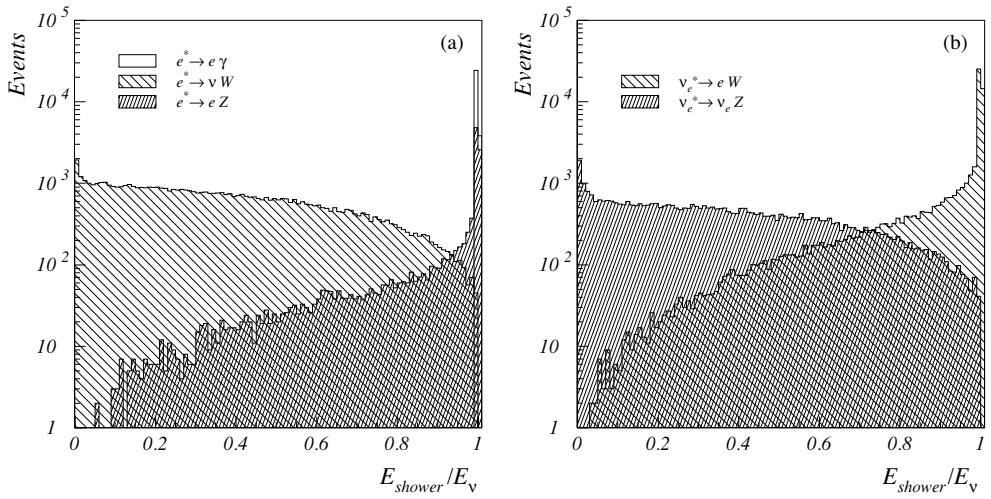

Figure 10. Ratio of the shower energy to the incident neutrino energy in the different decay modes of the excited lepton for (a) excited electron production and (b) excited electron neutrino production, with $f = f'$, $m_* = 1$ TeV/c^2 and $E_\nu = 10^{20}$ eV.

cycle). The acceptance of OWL was estimated from the aperture given in [5] for an altitude of 500 km.

In figure 9(b) the exposures of the different experiments are shown, which take into account both the acceptance and the effective observation time. The assumed observation periods are the ones described above (and quoted in the caption of the figure).

In the case of excited lepton production, $\nu N \to \nu^* X$ or $\nu N \to \ell^* X$, the relation between the shower energy and the incident neutrino energy is obtained from the $\mathrm{d}\sigma_{\nu N}/\mathrm{d}y$ distribution (see section 2.1, equation (5)) and depends on the decay mode of the produced neutral or charged excited lepton. The fraction of the incident neutrino energy carried away by the hadronic component X and thus, to some extent, the energy of the observable extensive air shower are determined by these distributions (such as the one in figure 3). On the other hand, the observability of the excited lepton decay products will depend on the decay mode.

Similarly, for leptoquarks, the actual shower energy will depend on the branching ratio and on the $\mathrm{d}\sigma_{\nu N}/\mathrm{d}y$ distribution. In the charged decay mode (see table 1) all the energy of the primary neutrino will contribute to the development of the extensive air shower. In the neutral decay mode, on the other hand, only the hadronic decay products will contribute.

For both excited leptons and leptoquarks, average values of the acceptance were computed via Monte Carlo in the way detailed below. For given values of the incident neutrino energy, the exotic particle mass and, in the case of excited leptons, the f, f' parameters, the production and decay were simulated taking into account the appropriate $\mathrm{d}\sigma_{\nu N}/\mathrm{d}y$ distributions and branching ratios. The models described in section 2 for excited lepton and leptoquark production and decay were implemented. The decay of any heavy gauge bosons arising from the exotic particle decay as well as the hadronization of the final state quarks was handled by JETSET [28]. For each set of input parameter values, one thousand events were generated for each exotic particle type (neutral and charged excited leptons of the three generations, and the leptoquarks listed in table 1). For each case, the shower energy was computed (as described in section 2.1.2). The ratio of the shower energy to the incident neutrino energy in the different decay modes of the excited leptons is shown for example cases in figure 10. The corresponding acceptances

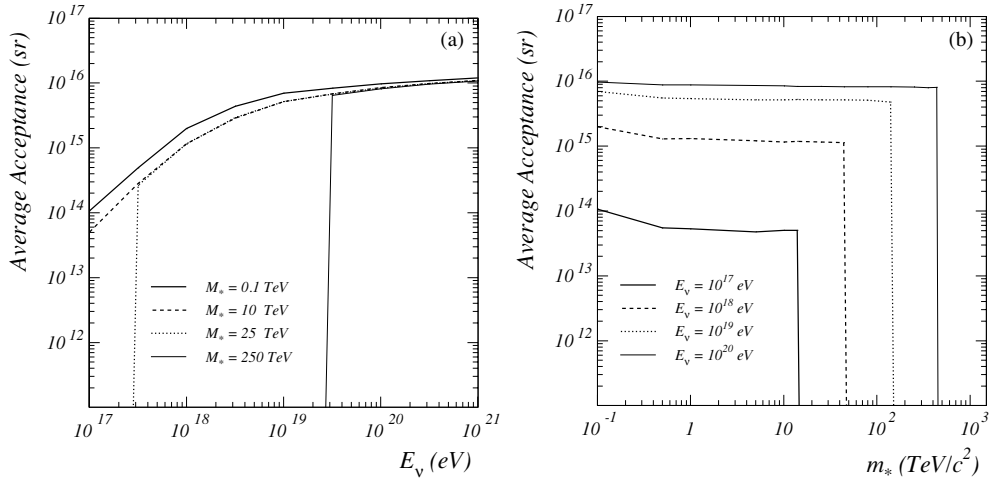

Figure 11. Average acceptance computed for Auger (a) as a function of the neutrino energy for different values of the excited lepton mass; (b) as a function of the excited lepton mass for different values of the incident neutrino energy. In this example, excited electron production with $f = f'$ was considered.

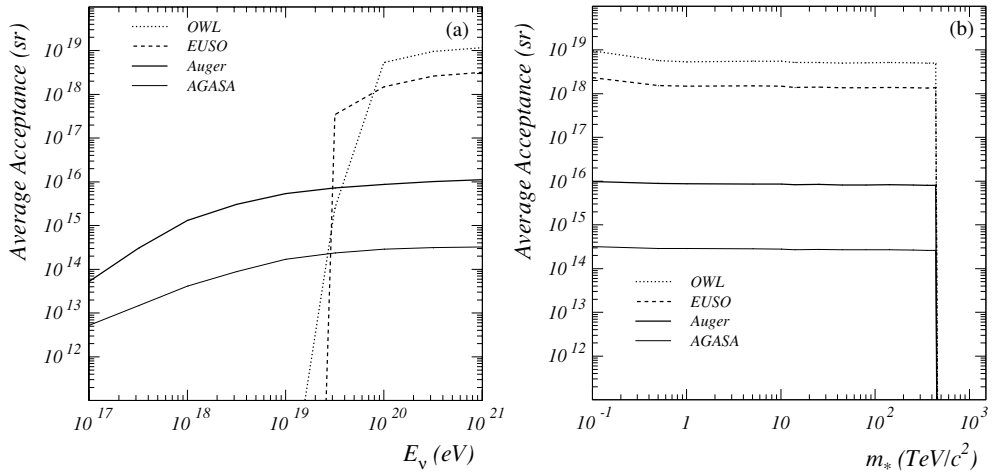

Figure 12. Average acceptances of the different experiments as a function of (a) the incident neutrino energy for $m_* = 1$ TeV/c^2; (b) the excited lepton mass, with $E_\nu = 10^{20}$ eV. These results are for excited electron production with $f = f'$.

were then obtained from figure 9. Averaging over all the generated events, an average acceptance was determined for each set of input parameters as a function of the incident neutrino energy. The average acceptance computed for Auger is shown in figure 11 as a function of the incident neutrino energy and of the excited lepton mass. It can be seen that while the kinematic limit effect is clearly visible, at higher energies the average acceptances follow relatively closely the one shown in figure 9. The average acceptances obtained for the different experiments are shown in figure 12, for $E_\nu = 10^{20} eV$ and $m_* = 1$ TeV/c^2. Again, the average acceptances are close to the ones shown in figure 9. This is due to the fact that

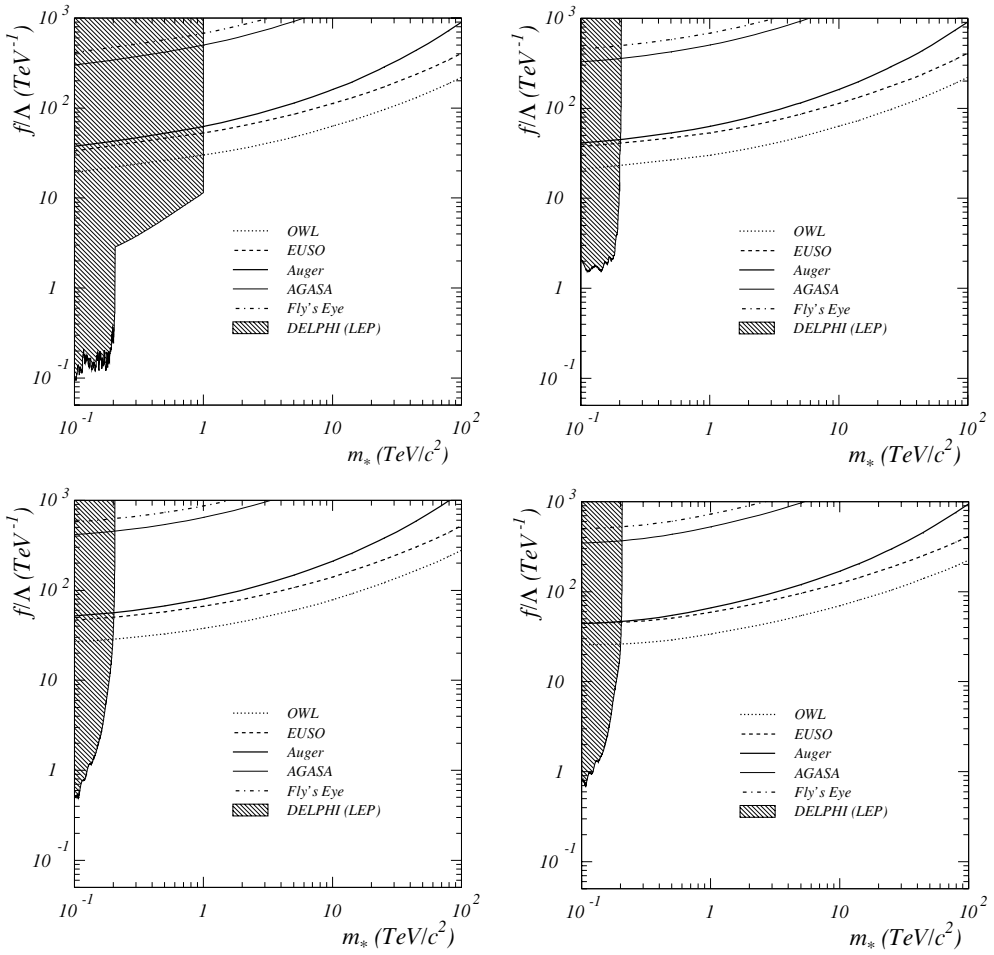

Figure 13. Estimated sensitivities of the different experiments as a function of the excited lepton mass for excited electrons (upper plots) and excited electron neutrinos (lower plots) in the scenarios $f = f'$ (left) and $f = -f'$ (right). The regions excluded by LEP are also shown (in dashed) for comparison. The observation times were taken as 10 years for Auger, 3 years and 10% duty cycle for both EUSO and OWL. For Agasa and Fly's Eye, the exposure was taken from [24].

in the dominant decay modes the fraction of the neutrino energy visible as shower energy is relatively high.

3.2. Results

Using equation (8), the sensitivity of the different experiments to excited lepton and leptoquark production as a function of the exotic particle mass was studied. Requiring the observation of one event, the sensitivity on the coupling as a function of the mass was derived.

3.2.1. Sensitivities for excited lepton production. Figure 13 shows the obtained sensitivities on the ratio f/Λ (see section 2.1) for first family excited leptons (excited electrons and excited electron neutrinos) as a function of the excited lepton mass, for the scenarios $f = f'$ and

$f = -f'$. The assumed observation times are the ones detailed above (and quoted in the caption of the figure). For comparison, limits on f/Λ obtained in direct and indirect searches for excited leptons at LEP are also shown [29]. LEP direct searches exclude f/Λ values down to below 1 TeV^{-1} in a mass range that extends up to about 200 GeV. Indirect searches, only applicable to excited electrons with non-vanishing electromagnetic coupling ($f = f'$ in our case), extend the exclusion to much higher masses, although with a poorer sensitivity.

These results show that, for the foreseen acceptances, observation time intervals and fluxes, cosmic ray experiments may detect excited lepton production only for rather large values of the coupling f/Λ. In this situation, they will nevertheless greatly extend the mass region explored at accelerators.

Excited leptons of different flavours, both charged and neutral, were also studied. The sensitivities obtained are, for these cases, comparable but slightly worse, due to the lower shower energy, for the same energy of the incident neutrino. The results obtained for third family excited leptons are shown in figure 14.

3.2.2. Sensitivities for first family leptoquarks. Figure 15 shows the sensitivity on the coupling λ as a function of the leptoquark mass expected in Auger, for different types of first family scalar and vector leptoquarks. As expected, better sensitivities are obtained for vector leptoquarks due to the larger cross sections. Other differences are due to coupling and branching ratio effects.

Figure 16 shows the expected sensitivities of the different cosmic ray experiments as a function of the leptoquark mass for first family scalar and vector leptoquarks. Limits obtained at accelerators are also shown. It can be seen that for first family leptoquarks the powerful limits obtained at LEP (L3 indirect search) and HERA (which include both direct and indirect searches at H1) exclude the region that could be probed at large cosmic ray experiments for the foreseen acceptances, observation time intervals and fluxes. As shown, low mass regions are also excluded by TEVATRON limits. Within the same family, the sensitivities for the different leptoquark types are within a factor of 2. The indirect limits of H1 and L3 were linearly extrapolated to higher masses. In the TeV region, however, leptoquark width effects were taken into account, making these limits weaker.

3.2.3. Sensitivities for second and third family leptoquarks. As discussed above, cosmic ray experiments would allow us to search for leptoquarks of all families, as the initial beam could contain all neutrino flavours. We can thus proceed to estimate the expected sensitivities for second and third family leptoquarks. These are shown in figure 17, for scalar leptoquarks, in the different considered experiments. In this case, most of the accelerator limits discussed above no longer apply, and cosmic ray experiments could play a role. The D0 limits shown in the figure correspond to scalar leptoquarks with both charged and neutral decay mode [9]. For third generation leptoquarks, the presently available limits are typically below 100 $\mathrm{GeV/c^2}$.

3.2.4. The double bang topology. For third family excited leptons and leptoquarks, an energetic tau lepton could be produced in the decay. In these cases, the double bang signature proposed in [12–14] could be searched for: the tau could travel long enough for its decay to produce a second shower, separate from the first one, but still within the field of view of the experiment. This rather distinctive new physics signature obviously requires a very large field of view, while the energy threshold for the observation of the second bang is also a critical issue. In fact, even for the experiments with the largest acceptances, only a few per cent of

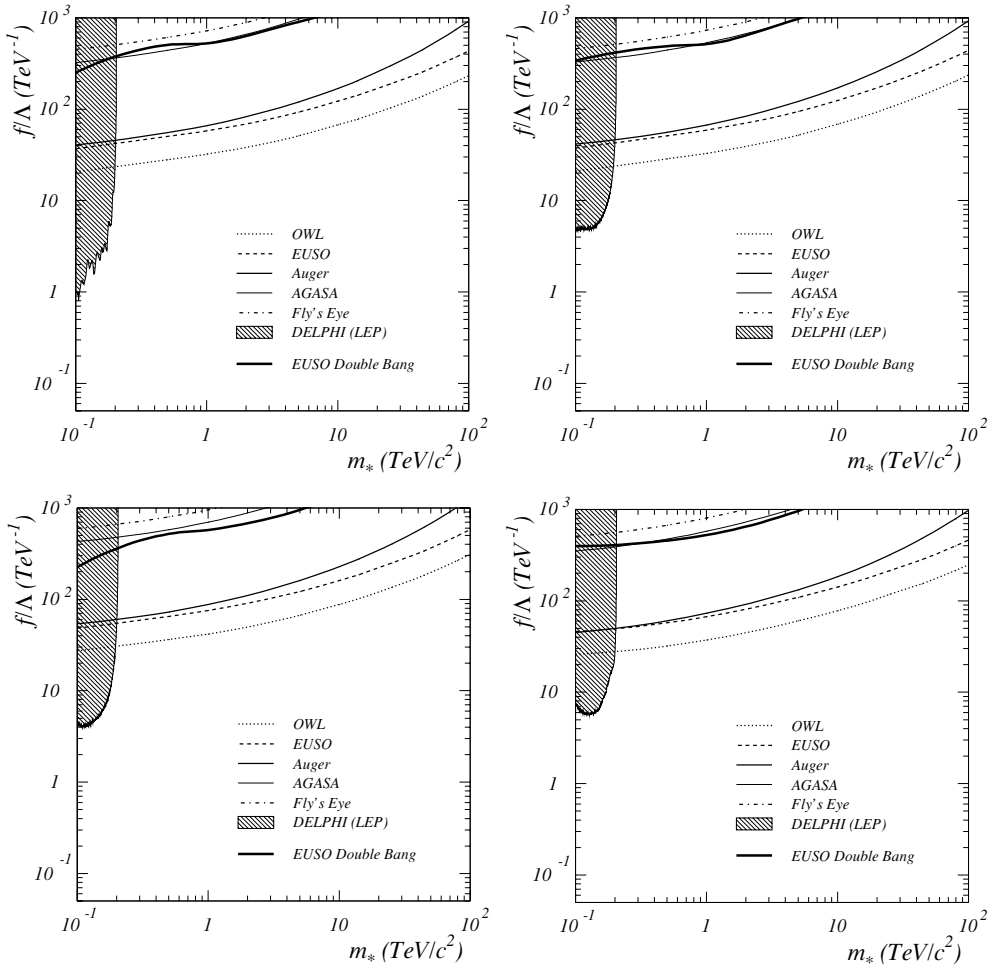

Figure 14. Estimated sensitivities of the different experiments as a function of the excited lepton mass for excited taus (upper plots) and excited tau neutrinos (lower plots) in the scenarios $f = f'$ (left) and $f = -f'$ (right). The regions excluded by LEP are also shown (in dashed) for comparison. The observation times were taken as 10 years for Auger, 3 years and 10% duty cycle for both EUSO and OWL. For Agasa and Fly's Eye, the exposure was taken from [24]. The sensitivity curves from double bang events in EUSO are also shown.

the detected events are expected to have a visible second bang. Using the procedure detailed in [14], the sensitivity from the observation of double bang events in EUSO was estimated. This curve is also shown in figures 14 and 17(b) for excited leptons and leptoquarks, respectively, where we see that we loose about one order of magnitude with respect to the sensitivity of the experiment. It should be noted that, in the case of double bang events, the sensitivity is determined by the interplay of competing effects: the energy of the second shower, which is the main limiting factor when it is relatively low, and the distance between the two showers, which may be too small for a good separation at moderate energies and will increase as the energy increases, eventually becoming too large, so that the second shower escapes detection.

The observation of a reasonable number of events could give some discriminating power between different new physics models expected to originate double bang events, based on

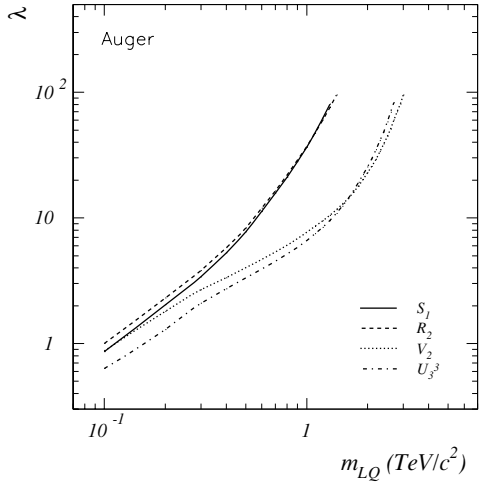

Figure 15. Estimated sensitivities of Auger for different first family leptoquarks as a function of the leptoquark mass for an observation period of 10 years.

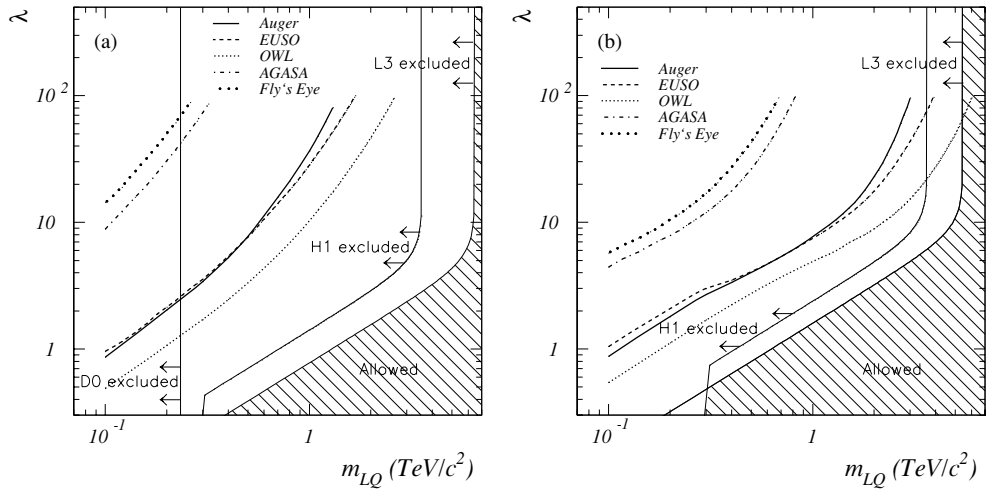

Figure 16. Estimated sensitivities of the different cosmic ray experiments for scalar S_1 (a) and vector V_2 (b) first family leptoquarks as a function of the leptoquark mass. The regions excluded by accelerator experiments are also shown for comparison. The observation times were taken as 10 years for Auger, 3 years and 10% duty cycle for both EUSO and OWL. For AGASA and Fly's Eye, the exposure was taken from [24].

the statistical comparison of the distributions of the three measured variables: the energies of the two showers and the distance between them, which are directly related to the production mechanisms and could provide some insight into these mechanisms. In the same way, a possible background arising from ν_τ regeneration on the atmosphere ($\nu_\tau \rightarrow \tau X$) [13], in itself a very interesting observation, could be identified taking into account that, in this case, contrary to what is expected in most of the considered new physics scenarios, the second shower is expected to be more energetic than the first one.

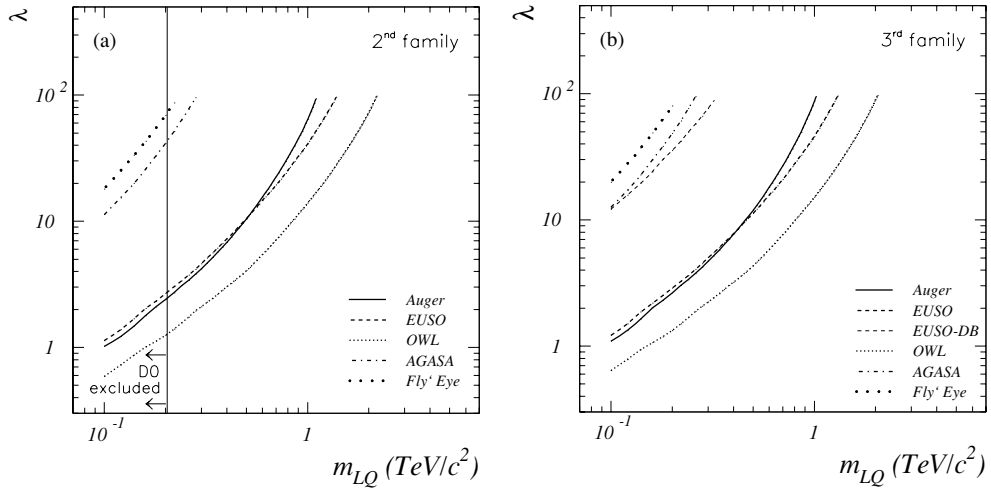

Figure 17. Estimated sensitivities of the different cosmic ray experiments for S_1 leptoquarks of second (a) and third (b) family leptoquarks as a function of the leptoquark mass. The observation times were taken as 10 years for Auger, 3 years and 10% duty cycle for both EUSO and OWL. For AGASA and Fly's Eye, the exposure was taken from [24]. In (b), the EUSO-DB line shows the expected sensitivity for double bang events (see text for details).

4. Conclusions

Excited leptons and leptoquarks are predicted in several new physics models and could be produced in the interaction of high energy quasi-horizontal cosmic neutrinos with the atmosphere. The possibility of detecting such exotic particles in present and future very high energy cosmic ray experiments was studied.

Effective models were used to compute interaction cross sections for the very high energy range and the results were cross-checked with references. Monte Carlo methods were used to estimate the average acceptances, as a function of the neutrino energy, taking into account the computed differential cross section and the exotic particle decay branching-ratios, as well as the neutrino acceptances of present and future very high energy cosmic ray experiments quoted in the literature [24, 25]. Sensitivity curves in the couplings as a function of the exotic particle mass were obtained for different experiments, assuming the Waxman–Bahcall bound for the neutrino flux, considering charged and neutral excited leptons and scalar and vector leptoquarks of the first, second and third family.

For excited leptons, the results show that cosmic ray air shower experiments may represent a window for searches in a mass range well beyond the TeV, if the coupling f/Λ is of the order of some tens of TeV^{-1}. For leptoquarks, while for the first family most of the coupling and mass ranges that could be probed in cosmic ray experiments have already been excluded by accelerator searches, relevant results could be obtained for second and third family leptoquarks.

These kinds of exotic particle production would, however, correspond only to an increase in the number of expected neutrino-induced horizontal showers. Although this is in itself a relevant prediction, the large uncertainties on the fluxes stress the need for complementary signatures, such as the double bang signature discussed above. In fact, double bang events could provide a distinctive signature, but only for very large acceptances or if the fluxes are larger than the ones considered. The discrimination of the different possible channels producing these kinds of signature would only be possible when some statistics is accumulated

taking into account the distributions of the energy of the two showers and of the distance between them.

Acknowledgment

The work of BT is supported by FCT grant SFRH/BPD/11547/2002.

References

[1] Takeda M *et al* 1998 *Phys. Rev. Lett.* **81** 1163 (*Preprint* astro-ph/9807193)
Hayashida N *et al* 2000 *Preprint* astro-ph/0008102, http://www.akeno.icrr.u-tokyo.ac.jp/AGASA
[2] Bird D J *et al* 1993 *Phys. Rev. Lett.* **71** 3401
Bird D J *et al* 1994 *Astrophys. J.* **424** 491
Bird D J *et al* 1995 *Astrophys. J.* **441** 144 (*Preprint* astro-ph/9410067)
[3] Auger Collaboration 1996 *The Pierre Auger Project Design Report* FERMILAB-PUB-96-024, 252, http://www.auger.org
[4] Catalano O 2001 *Nuovo Cimento* C **24** 445 http://www.euso-mission.org
Scarsi L *et al* (EUSO Collaboration) 2003 Report on the EUSO Phase A study *EUSO Report* EUSO-PI-REP-002-1
[5] Krizmanic J F *et al* (OWL/AirWatch Collaboration) 1999 *Proc. 26th Int. Cosmic Ray Conf.* vol 2, p 388, http://owl.gsfc.nasa.gov
[6] Hagiwara K, Zeppenfeld D and Komamiya S 1985 *Z. Phys.* C **29** 115
Boudjema F, Djouadi A and Kneur J L 1993 *Z. Phys.* C **57** 425
Djouadi A 1994 *Z. Phys.* C **63** 317
[7] Buchmuller W, Ruckl R and Wyler D 1987 *Phys. Lett.* B **191** 442
[8] DELPHI Collaboration 1999 *Eur. Phys. J.* C **8** 41
Abbiendi G *et al* (OPAL Collaboration) 2002 *Phys. Lett.* B **544** 57
Achard P *et al* (L3 Collaboration) 2003 *Phys. Lett.* B **568** 23
Medcalf T *et al* (ALEPH Collaboration) CERN-OPEN 99-171, contributed paper to *EPS-HEP 99*
Adloff C *et al* (H1 Collaboration) 2002 *Phys. Lett.* B **548** 35
Adloff C *et al* (H1 Collaboration) 2002 *Phys. Lett.* B **525** 9
Chekanov S *et al* (ZEUS Collaboration) 2002 *Phys. Lett.* B **549** 32
Abe F *et al* (CDF Collaboration) 1994 *Phys. Rev. Lett.* **72** 1977
CDF Collaboration 2004 CDF note 7177, contributed paper to *ICHEP2004 (Beijing, Aug.)*
[9] Adloff C *et al* (H1 Collaboration) 2003 *Phys. Lett.* B **568** 35
H1 Collaboration 2005 *Preprint* hep-ex/0506044
Acciarri M *et al* (L3 Collaboration) 2000 *Phys. Lett.* B **489** 81
Abbiendi G *et al* (OPAL Collaboration) 1999 *Eur. Phys. J.* C **6** 1
Abreu P *et al* (DELPHI Collaboration) 1999 *Phys. Lett.* B **446** 62
Abazov V M *et al* (D0 Collaboration) 2005 *Phys. Rev.* D **71** 071104
Grosso-Pilcher C *et al* (CDF and D0 Collaborations) 1998 *Preprint* hep-ex/9810015
Abbott B *et al* (D0 Collaboration) 1997 *Phys. Rev. Lett.* **79** 4321
Abe F *et al* (CDF Collaboration) 1997 *Phys. Rev. Lett.* **79** 4327
D0 Collaboration D0 Note 4829
[10] Halzen F and Hooper D 2002 *Rep. Prog. Phys.* **65** 1025 (*Preprint* astro-ph/0204527)
Kalashev O E, Kuzmin V A, Semikoz D V and Sigl G 2002 *Phys. Rev.* D **66** 063004 (*Preprint* hep-ph/0205050)
[11] Tyler C, Olinto A V and Sigl G 2001 *Phys. Rev.* D **63** 050001 (*Preprint* hep-ph/0002257)
Ringwald A 2004 Invited talk at *CRIS2004 (Catania, May)* (*Preprint* hep-ph/0409151)
[12] Fargion D *et al* 1997 *Preprint* astro-ph/9704205
Fargion D *et al* 2003 *Preprint* hep-ph/0305128
Bottai S and Giurgola S 2003 *Astropart. Phys.* **18** 539 (*Preprint* astro-ph/0205325)
Guzzo M M and Moura C A Jr 2003 *Preprint* hep-ph/0312119
[13] Athar H, Parente G and Zas E 2000 *Phys. Rev.* D **62** 093010 (*Preprint* hep-ph/0006123)
[14] Cardoso V, Espirito Santo M C, Paulos M, Pimenta M and Tome B 2005 *Astropart. Phys.* **22** 399
[15] Barnett R M 1976 *Phys. Rev.* D **14** 70

[16] Pumplin J, Stump D R, Huston J, Lai H L, Nadolsky P and Tung W K 2002 *J. High Energy Phys.* JHEP07(2002)012 (*Preprint* hep-ph/0201195)
Stump D, Huston J, Pumplin J, Tung W K, Lai H L, Kuhlmann S and Owens J 2003 *J. High Energy Phys.* JHEP10(2003)046 (*Preprint* hep-ph/0303013)
Kretzer S, Lai H L, Olness F and Tung W K 2004 *Phys. Rev.* D **69** 114005 (*Preprint* hep-ph/0307022)
[17] Reno M H 2004 *Preprint* hep-ph/0410109
[18] Gandhi R, Quigg C, Reno M H and Sarcevic I 1998 *Phys. Rev.* D **58** 093009 (*Preprint* hep-ph/9807264)
[19] Brasse F W *et al* 1972 *Nucl. Phys.* B **39** 421
[20] Anchordoqui L A, Fodor Z, Katz S D, Ringwald A and Tu H 2004 *Preprint* hep-ph/0410136
Tu H 2004 *PhD Thesis* DESY and University Hamburg, DESY-THESIS-2004-018
[21] Waxman E and Bahcall J N 1999 *Phys. Rev.* D **59** 023002 (*Preprint* hep-ph/9807282)
Waxman E and Bahcall J N 1999 *Preprint* hep-ph/9902383
[22] Mannheim K, Protheroe R J and Rachen J P 2001 *Phys. Rev.* D **63** 023003 (*Preprint* astro-ph/9812398)
[23] Berezinsky V S and Smirnov A Y 1974 *Phys. Lett.* B **48** 269
[24] Anchordoqui L A, Feng J L, Goldberg H and Shapere A D 2002 *Phys. Rev.* D **66** 103002 (*Preprint* hep-ph/0207139)
[25] Capelle K S, Cronin J W, Parente G and Zas E 1998 *Astropart. Phys.* **8** 321 (*Preprint* astro-ph/9801313)
Anchordoqui L A, Feng J L, Goldberg H and Shapere A D 2002 *Phys. Rev.* D **65** 124027 (*Preprint* hep-ph/0112247)
Anchordoqui L A, Feng J L, Goldberg H and Shapere A D 2001 *Auger Internal Note GAP-2001-053*
[26] Bottai S and Giurgola S (EUSO Collaboration) 2003 *Proc. 28th Int. Cosmic Ray Conf. (ICRC 2003) (Tsukuba, Japan, 31 July–7 Aug.)* p 1113
[27] Dutta S I, Reno M H and Sarcevic I 2002 *Phys. Rev.* D **66** 033002 (*Preprint* hep-ph/0204218)
[28] Sjostrand T, Eden P, Friberg C, Lonnblad L, Miu G, Mrenna S and Norrbin E 2001 *Comput. Phys. Commun.* **135** 238
Sjostrand T 1994 *Comput. Phys. Commun.* **82** 74
[29] Adam W *et al* 2004 DELPHI 2004-024 CONF 699, contributed paper to *ICHEP2004 (Beijing, August)*